CHAPTER 4

Electrochemical studies on Self-Assembled Monolayers of some Dithiols, Hydroxy, Carboxylic acid and amino thiols on gold

4.0 Introduction :

Self-assembled monolayers of alkanethiols form a (□3Δ□3) R 30° overlayer structure on Au (111) surfaces. The monolayers provide an ideal model system for studying a large variety of interfacial phenomena, which are difficult to study in natural interfaces. Organic disulphides [1,2], thiols [3,4], sulphides [5] on gold surfaces and carboxylic acids [6] and silanes [7] on various oxide surfaces have been utilized extensively as model systems in recent times. Among various interfacial phenomena, long range electron transfer can provide useful information in biological research. In the recent times, various groups [3,4,8,9] have shown interest in the studies of interfacial electron transfer between a metal electrode and a molecular donor or acceptor using alkanethiol coated gold as the model system. Electrochemical measurements show that the long chain n-alkane monolayers are impermeable to ions in contacting aqueous electrolyte solution [3]. The films act like dielectrics of definite thickness and dielectric constant. In addition to this, very low electron-transfer currents are observed with electron acceptors in the contacting solution. Different electron donors

or acceptors can be attached with the functional groups at the outer surface (terminal groups) of the monolayer to study the electron transfer phenomena. In this context, the monolayer in which the terminal group substituted by electroactive group is of fundamental interest in view of the electron transfer process through the controlled distance between the electron donor and acceptor [10-12]. On the other hand, the monolayers of electroinactive but polar terminal groups are also interesting due to the effect of these terminal groups on the electrochemical responses of the species in solution [13-15]. The terminal polar groups may be neutral or ionic. Due to the strength of the interaction of thiols with gold, many polar functional groups can be included in the adsorbate without changing the adsorption of the thiol group to the gold surface. Different experimental data have given evidence to the fact that the terminal groups of ω-substituted alkanethiol monolayers are located at the outer surface as expected [15-17]. However, the presence of different functional groups at the outer surface may affect the structure and orientation of the monolayer. For example, if the size of functional groups set the spacing of the chains, a greater tilting is expected than the unsubstituted alkanethiols. Chidsey and Loiacono [18] have studied the structural and electrochemical properties of alkanethiol monolayers $HSC_{10}X$, X=H, CH_2OH, CN, COOH with very simple functional groups at their outer surface. They have examined the defect properties and permeability of monolayers of long-chain organic molecules bound to gold electrode in aqueous medium. The defect and pinhole currents for redox couples and their interfacial capacitances increase in the order H < CH_2OH < CN < COOH. They found that there was no clear correlation of the permeability of monolayers with their wettability and structure. For

example, SAM with a hydrophilic surface ($X=CH_2OH$) is more blocking than one with a hydrophobic surface (X=CN).

However, we find from literature there have been no studies on the barrier properties, structural integrity, stability and orientation of alkanethiol SAMs with different functional groups in different non-aqueous solvents. This may be primarily due to their perceived instability in these solvents. However, we find that this conclusion is due to the insufficient understanding of the electron transfer properties in these solvents. We have studied [19,20] the stability and structural integrity of unsubstituted n-alkanethiol monolayers and correlated them with the bulk structure of some non-aqueous solvents using ferrocene as the redox probe. In this chapter, we report our results on the barrier properties of different alkanethiol derivatives like hydroxy and carboxylic acid thiols in different non-aqueous solvents like acetonitrile, propylene carbonate, formamide and ethanol.

Organic dithiol monolayers provide the basis for the design of molecular wires capable of bridging between proximate gold surfaces in future molecular electronics devices [21-24] and as such it is quite important to understand the structural integrity, orientation, and barrier properties of such organic dithiol monolayers in aqueous and non-aqueous solvents. We find from literature that several groups have studied structure and orientation of dithiol molecules on Au and Ag. For example, Brust et al. [25] reported that multilayer structures of copper ions sandwiched between dithiol molecules can be formed using 1,6-hexanedithiol. They suggested from their ellipsometry measurements that the first monolayer of dithiols is adsorbed to the gold surface with only one of the –SH groups resulting in layer by layer growth. Riley et al. [26] used XPS to study the structure of octanedithiol SAMs on gold. The data were found to be consistent with a structure with

vertical orientation. On the basis of their STM observations, Nakamura et al. [27] have reported a similar upright configuration for 1,12-dodecanedithiol and a thiophene containing dithiol monolayer on gold. But it is rather surprising to see Kobayashi et al. [28] have reported that octanedithiol molecules are aligned with their axes parallel to Au (111) surface from their study on the structure of SAM of octanedithiol molecules using ultrahigh vacuum STM. Their results contradict the results of the other groups [25-27]. We find from literature that there has been no reports of electrochemical studies on the barrier properties and structural integrity of organic dithiols in any non–aqueous solvent. Hence, we have undertaken studies on the ferrocene electron transfer reaction through self-assembled monolayers of aliphatic and aromatic dithiols SAMs on gold in acetonitrile, a commonly used aprotic solvent [29]. Since interfacial capacitance measurements have been effectively utilised by various groups to precisely determine the monolayer thickness and orientation of alkanethiol SAMs, we have also used this technique to determine the thickness, orientation, permeability of hexanedithiol, octanedithiol and 1,4 benzenedimethanethiol on gold [29].

With the exception of the SAMs with terminal COOH groups, the blocking SAMs are uncharged. The blocking behaviour can be dramatically affected by the introduction or creation of charge sites on the external surface of the monolayer. Various theoretical studies [30-32] on the surface potential of the SAM with ionic terminal group show that there is changes in ϕ_{DL} on the order of 100 mV due to ionization of the terminal group (e.g., $Au/SC_nCOOH \rightarrow Au/SC_nCOO^-$) in concentrated electrolyte. The concentration of an ionic redox molecule with charge z at the SAM is related to the surface potential ϕ_{DL} by the relation $C_s = C_b \exp(-zF\phi_{DL}/RT)$, where

C_s and C_b are the surface and bulk concentration of the redox species. Therefore, ionization of terminal groups can be observed by following the barrier property of the SAM towards a charged redox couple. Hanshew and Finklea have studied the blocking behaviour of $HSC_{10}COOH$ and pendant pyridine SAMs to $Ru(NH_3)_6^{+3}$ as a function of electrolyte pH [33]. The $HSC_{10}COOH$ SAM at low pH is sufficiently blocking to Ru(III) ions. However, cathodic current for Ru(III) increases as the pH of the solution is enhanced to a value of 5, and both the anodic and cathodic peaks are visible at pHs 6 to 8. Lowering the pH reverses the block behaviour, indicating the SAM is not desorbed or damaged. The SAM with pendant pyridine exhibits the same behaviour as $HSC_{10}COOH$ SAM, but for the opposite reason. Ru(III) reduction current decreases as the pH is lowered, but increases as the pH reaches a higher value. Protonation of the pyridines appears to start by pH 7 and continues to pH 4 or 5.

In order to understand the effect of surface charge on the barrier property of ionic SAMs towards ionic electroactive species, we have studied the barrier properties of SAMs of 11-mercapto undecanoic acid and 4-amino thiophenol on gold using ferrocyanide and hexaammine ruthenium (III) chloride as redox probe molecules at different pH values of electrolytic solution.

4.1 Experimental :

4.1.1Electrodes and cells

Gold working electrode was constructed by proper sealing of 99.99% pure gold wire (Arora Mathey) of 0.5 mm diameter with soda lime glass having thermal expansion coefficient close to that of gold. The electrode has a

geometric area of 0.002 cm^2. This small area working electrode has highly reproducible true surface area (as measured by potential cycling in 0.1M perchloric acid) even after repeated usage.

A conventional three electrode electrochemical cell was used in this study. A platinum foil of large surface area was used as counter electrode. A saturated calomel electrode (SCE) was used as reference electrode in ethanol medium, whereas a silver rod was used as a quasi-reference electrode in acetonitrile [34,35] propylene carbonate, formamide and other non-aqueous solvents. The silver quasi-reference electrode has a potential of –0.2 V with respect to saturated calomel electrode (SCE) [36] in acetonitrile. This electrode has a stable potential in non-aqueous solvents and also is free of any liquid junction potential. For experiment in ethanol, an electrochemical cell with a provision for SCE in a separate compartment connected by a Luggin capillary was used. Evaporated gold substrates on glass were used as working electrode in some of our studies. Evaporation of gold (~100 nm thickness) on glass was carried out using vacuum evaporation unit (Hindhivac) at a pressure of 2×10^{-5} mbar. Chromium underlayers (2-5 nm thickness) were deposited on glass before gold evaporation to improve the adhesion of gold on glass. The substrate was heated to 350 ^{0} C during gold evaporation, a process which normally yields a substrate with predominantly Au (111) orientation. The gold samples were used as strips for electrochemical studies with a well defined area exposed to the electrolyte solution, rest of the portion being insulated with parafilm and teflon. These gold samples were cleaned with Piranha solution (mixture of concentrated sulphuric acid and 30% hydrogen peroxide in 3:1 ratio) for 30 s before each experiment and finally rinsed in millipore water. Before each experiment, the electrolyte was completely deaerated by passing oxygen free nitrogen

gas. During the experiment, a blanket of nitrogen gas was maintained on top of the solution. The cell was cleaned thoroughly before each experiment and kept in a hot air oven at 100^0C for at least one hour before the start of the experiment.

4.1.2 Electrode pretreatment and thiol adsorption

Immediately before use, the gold electrode was polished using aqueous slurries of progressively finer alumina (1.0, 0.3 and 0.05 μm sizes), sonicated to remove alumina particle and finally etched using dilute aqua regia (3:1:4 ratio of concentrated HCl, concentrated HNO_3 and water) for one minute. This procedure had been shown to yield a substrate with the best blocking properties for supporting self-assembled monolayer of alkanethiols [11,12]. We have conducted experiments where the monolayer is formed by dipping the electrode in 1 mM ethanolic solution for 24 hours. Monolayers were also prepared from neat 11 mercapto 1-undecanol and 11-mercapto undecanoic acid at 40^0 C and 50^0C in a thermostat for 1 hour as they are solids at room temperature.

4.1.3 Instrumentation

Cyclic voltammetry was carried out using an EG&G potentiostat (Model 263A) interfaced to a PC through a GPIB card (National Instruments). The potential ranges and scan rates used are shown in the respective figures. Electrochemical impedance studies were performed using an EG&G potentiostat (Model 263A) along with a two phase lock-in amplifier (Stanford Research Systems Model SR 830). A pure sine wave of 10 mV amplitude was derived from the lock- in amplifier for application to the cell. Impedance studies were carried out at formal potential of the respective systems as measured from the cyclic voltammograms. The capacitance values presented here are for true area after accounting for the roughness

factor of 1.5 for the substrate measured from the oxide stripping peak by potential cycling in 0.1 M perchloric acid. The impedance data in acetonitrile were analyzed using the ZsimpWin EIS DATA analysis software (Perkin Elmer, version 2.00) by fitting to an appropriate equivalent circuit. The IR spectra were obtained using FT-IR 8400 model (SHIMADZU) with a fixed 85^0 grazing angle attachment (FT-85; Thermo Spectra-Tech).

4.1.4 Chemicals

Ethanol 99.95% (Emerck), hexanedithiol, octanedithiol, 1,4 benzenedimethanethiol, 11-mercapto 1-undecanol, 11-mercapto undecanoic acid, 4-amino thiophenol (Aldrich), tetrabutylammonium tetrafluroborate (Aldrich), lithium perchlorate (Fischer), ferrocene (Acros Organics), perchloric acid (Qualigens), acetonitrile (Ranbaxy), propylene carbonate (Spectrochem), formamide (SRL), potassium ferrocyanide (Loba), sodium fluoride (Qualigens), sulphuric acid (Qualigens), sodium hydroxide (BDH), hexaammine ruthenium (III) chloride (Alfa Aesar) were used in our studies. Millipore water was used for making aqueous solution.

4.2 Results and discussion :

4.2.1 Determination of orientation of dithiol SAM

The capacitance of the monolayer is related to its dielectric constant and thickness by the relationship based on Helmholtz model: $C = \frac{\varepsilon \varepsilon_0}{d}$ where ε is the dielectric constant of the alkanethiol molecule, ε_0 is the permittivity of free space and d is thickness of the monolayer. The capacitance value thus depends inversely on the thickness of the monolayer. A change in the thickness of the monolayer should manifest itself by a corresponding change in capacitance. Hence, measurement of capacitance is a very sensitive method to measure the thickness of SAMs. For example, during the self -

assembly process, the alkanedithiol can adsorb with both the sulphur atoms bonded with gold or alternatively with only one sulphur atom chemisorbed onto gold as it happens in the case of simple alkanethiols. If the octanedithiol molecule is aligned with its axis parallel to the Au surface (both S atoms chemisorbed on gold) then its capacitance would be expected to be much higher than when it is adsorbed vertically or with some tilt angle.

Table 1 shows the interfacial capacitance values of the three thiols, namely hexanedithiol, octanedithiol and 1,4 benzenedimethanethiol (BDMT) modified gold electrodes in 1 M NaF in water by cyclic voltammetry and impedance spectroscopy.

Table 1

capacitance values for different dithiol coated Au electrodes using cyclic voltammetry and impedance spectroscopy

DITHIOL	C / μF cm^{-2} (from CV)	C / μF cm^{-2} (from Z)
Hexanedithiol	2.82	2.85
Octanedithiol	2.60	2.67
1,4 benzenedimethanethiol	2.50	2.45

The capacitance of octanedithiol monolayer for a full monolayer coverage is 2.67 $\mu F\ cm^{-2}$, while that of octanethiol is 2.45 $\mu F\ cm^{-2}$. Since, both the thiols have comparable chain lengths and the measured capacitance values are also quite close, we can infer that octanedithiol adsorbs with only one sulphur atom onto gold. The small difference in capacitance values between octanethiol and octanedithiol could be attributed to different tilt angles of these two thiols. The capacitance values obtained for hexanedithiol

and BDMT also correspond to the vertical orientation of dithiol molecules on gold.

4.2.2 FT-IR Spectroscopic studies of dithiol SAMs

We have carried out grazing angle FT-IR spectroscopy on SAMs of octanedithiol (ODT) and 1,4 benzenedimethanethiol (BDMT). Figure 1 A shows the C-H region in the IR spectrum of 1 mM ODT coated Au surface. The peaks at 2918 and 2851 cm^{-1} are the asymmetric and symmetric C-H stretching modes of CH_2 group. The C-H stretching vibrations of the alkyl chain are very sensitive to packing density and to the presence of gauche defects, which makes them ideally suited as probes to determine the SAM quality [3]. In particular, the asymmetric CH_2 stretching vibration at 2918 cm^{-1} is a useful indicator for SAMs of exceptional quality. Hence, our IR results indicate the formation of high quality ordered SAM in 1 mM ODT. One important distinguishing feature of IR spectra of octanedithiol SAM *vis- a -vis* the alkanethiol SAM is the absence of peaks at 2878 and 2964 cm^{-1} due to absence of $-CH_3$ terminal group. Figure 1 B shows the C-H region in the IR spectrum of 1 mM BDMT coated Au surface. Multiple peaks between 3100 to 3000 cm^{-1} correspond to aromatic C-H stretching modes of the phenyl ring. The peak at 2922 cm^{-1} corresponds to the asymmetric C-H stretching modes of CH_2 group. However, if the aromatic phenyl rings are perpendicular to the surface, then peak due to 8a and 8b skeletal vibrations (Wilson's notation) should be observed at 1609 cm^{-1}. But, we have excluded that part of spectrum because of the poor quality of spectrum in this region due to noise.

4.2.3 Study of barrier properties of dithiol coated Au in acetonitrile

Figure 2 shows the cyclic voltammogram of ferrocene redox reaction on bare Au disk electrode (a) and 1 mM octanedithiol coated electrode (b) in acetonitrile containing 0.1 M TBAFB. The first cycle CV of 1 mM octanedithiol coated electrode exhibits a partial blocking behaviour (not shown in the figure). As scanning continues however, we get voltammogram with characteristics of quasi-reversible redox reaction (Figure 2 b). In order to check whether there is any desorption of thiol monolayer that might have occurred during potential cycling in acetonitrile, we have carried out the following experiments with the same electrode, which was previously scanned in acetonitrile.

(3) CV of $Fe(CN)_6^{3-}$ | $Fe(CN)_6^{4-}$ in 1 M KCl in water.

(4) Electrochemical desorption of octanedithiol monolayer by cycling to very negative potential (below –1.0 V vs SCE) in acetonitrile, followed by CV of $Fe(CN)_6^{3-}$ | $Fe(CN)_6^{4-}$ in 1M KCl.

In the above study, we have used $Fe(CN)_6^{3-}$ as a redox probe to evaluate the integrity of SAM.

Figure 3a shows the CV of ferrocyanide redox reaction on bare gold electrode in 1M KCl in water, which has the usual characteristics of a reversible redox reaction, while Figure 3b shows the voltammogram of octanedithiol coated electrode for ferrocyanide redox reaction, which was previously subjected to potential scanning in acetonitrile. It can be seen that this electrode exhibits very good blocking to ferrocyanide redox reaction, which is a clear indication that octanedithiol molecules have not desorbed during the potential scanning in acetonitrile.

This is further proved by another experiment; We have scanned the potential to a very negative value (below –1.0 V vs SCE) in acetonitrile, as

it is known that the thiol monolayer undergoes reductive desorption at such an extreme negative potential. It can be seen from the desorption peak that the octanedithiol monolayer was very much intact during the earlier potential scanning in acetonitrile. After the desorption of dithiol monolayer, again a CV of ferrocyanide redox reaction was carried out on the same electrode. Figure 3c shows that the CV so obtained, has features very much similar to that of bare gold electrode. This proves that alkanethiol monolayer has not disintegrated, but somehow allows the ferrocene electron transfer. The above series of experiments prove that octanedithiol monolayer was stable in acetonitrile medium within the potential range of scanning, but undergoes some kind of disorganization which results in significant faradaic current during ferrocene redox reaction. These results are very much in agreement with our previous studies on the barrier properties of alkanethiol SAMs in different non-aqueous solvents [19]. The mechanism of electron transfer across a disorganized SAM in acetonitrile has been discussed in details in Chapter 3.

Figure 2 (c) shows the cyclic voltammogram of 1 mM BDMT coated Au electrode for ferrocene redox reaction in acetonitrile. It can be seen that BDMT coated Au surface exhibits better blocking properties compared to ODT coated Au electrode even after continuous scanning in a solvent like acetonitrile which is known to disorganise alkanethiol SAMs [19]. This can be attributed to the strong lateral van der Waals interaction among the phenyl rings of BDMT molecules on gold surface. As a result, BDMT molecules can form more well organized monolayer on gold compared to aliphatic octanedithiol molecules. Infact, the monolayer formed by BDMT is much more organised in this solvent than even alkanethiol monolayers [19].

4.2.4 Electrochemical impedance studies

Figure 4 A shows the Nyquist plot of bare gold disk electrode carried out at a potential of +0.30 V vs SCE for 1 mM ferrocene + 1 mM ferricenium in acetonitrile containing 0.1 M tetrabutylammonium tetrafluroborate as supporting electrolyte. It can be seen that the reaction is diffusion controlled for almost the whole frequency range of 0.1 Hz to 30 kHz showing a fast charge transfer reaction.

Figure 4 B shows the impedance plot for the same electrode after adsorption in 1 mM octanedithiol in ethanol for 24 hours.The small semicircle at very high frequencies reveals a charge transfer process, while the reaction is very much diffusion controlled for the rest of the frequency range. This supports the CV results of Figure 2 (b) which shows a peak separation of 100 mV corresponding to a quasi-reversible charge transfer process. However, it can be seen from Figure 4 C that for 1 mM BDMT coated Au electrode, a larger semicircle upto the mid frequency region corresponding to charge transfer controlled process is obtained. At very low frequencies, however, the effect of mass transfer still persists. This again confirms the CV results (Figure 2 c) which shows a S-shaped voltammogram corresponding to completely irreversible charge transfer process. The R_{ct} for ferrocene redox reaction obtained from the fitting of impedance data for 1 mM BDMT coated Au electrode (R_{ct} =157.58 Ω cm^2) is 10 times greater than the 1 mM ODT coated Au electrode (R_{ct} =16.65 Ω cm^2). The above impedance results are quite consistent with the conclusions arrived at after CV experiments that the monolayer formed in BDMT has a much better barrier property than the one formed in octanedithiol towards ferrocene redox reaction in acetonitrile.

4.2.5 Equivalent circuit analysis of impedance data

There has been no report in literature of the equivalent circuit modeling of impedance data of alkanethiol SAMs in non-aqueous medium in the presence of some redox species. In this chapter, we model the interface of octanedithiol and 1,4 benzene dimethanethiol coated Au disk electrode for ferrocene redox reaction in acetonitrile to a Randle's type equivalent circuit. Tables 2 and 3 show the values of different components, viz., R_u, R_{ct}, C_{dl}, Q and W obtained by fitting the impedance data to different equivalent circuits (The equivalent circuits are shown at the top of the respective tables). When the data are fitted to the equivalent circuit model R(C(RW)), the capacitance value obtained is very large for a monolayer film and the fitting is also very poor with large error. However, it can be seen from Table 3, that when the capacitance C is replaced by constant phase element Q in the equivalent circuit R(Q(RW)) the impedance data fits very well.

As the impedance of the CPE is given by $Z_{CPE} = 1/ Q(j\omega)^n$, when n = 1, a purely capacitive behaviour is expected (i.e. $Q = C_{dl}$). The values of n in the case of octanedithiol and BDMT are 0.66 and 0.72 respectively, which indicates that there is a large deviation from purely capacitive behaviour. The CPE has no definite physical significance and does not represent any specific interfacial process [37,38]. However, it is helpful in the analysis of impedance data affected by frequency dispersion. For instance the perturbation to purely charge transfer process caused by deep pores or rough surfaces can be represented in terms of CPE. In our impedance analysis, the deviation from the capacitive behaviour as represented by constant phase element Q is brought about by the disorganisation introduced by the acetonitrile molecules on the organic thiol monolayer.

Table 2

Values of different components of the equivalent circuit R(C(RW)) obtained from the fitting of impedance data for ferrocene redox reaction in acetonitrile

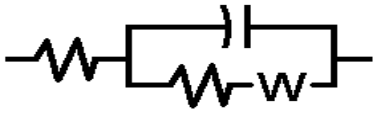

Dithiol	R_u /Ω cm^2	C_{dl}/ F cm^{-2}	R_{ct} / Ω cm^2	W/Ω cm^2
1 mM ODT coated Au	2.04	2.67×10^{-5}	6.54	6.79×10^{-3}
1 mM BDMT coated Au	2.86	3.54×10^{-6}	110.54	3.24×10^{-3}

Table 3

Values of different components of the equivalent circuit R(Q(RW)) obtained from the fitting of impedance data for ferrocene redox reaction in acetonitrile

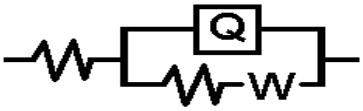

Dithiol	R_u /Ω cm^2	Q/Ω^{-1} cm^{-2} s^n	*n*	R_{ct} / Ω cm^2	W/Ω cm^2
1 mM ODT coated Au	1.66	6.43×10^{-4}	0.66	16.65	7.04×10^{-3}
1 mM BDMT coated Au	1.31	5.87×10^{-5}	0.72	157.58	4.34×10^{-3}

The ferrocene redox reactions in acetonitrile in the presence of insulating ODT and BDMT SAMs on gold can take place by either diffusion of the ferrocene molecules through the pinholes and access to the electrode

surface followed by electron transfer reaction or permeation of ferrocene molecules through the disorganised assembly and access to the region closer to the electrode surface followed by electron transfer by tunneling .

4.2.6 Effect of some non-aqueous solvents on the barrier properties of hydroxy and carboxylic acid thiol SAMs

<u>11-mercapto 1-undecanol</u>

acetonitrile and propylene carbonate

Figure 5 shows the cyclic voltammogram of ferrocene redox reaction on bare Au electrode (a) and neat 11-mercapto 1-undecanol coated electrode (b) in acetonitrile containing 0.1 M TBAFB. The first cycle CV of neat 11-mercapto 1-undecanol coated electrode exhibits a partial blocking behaviour (not shown in the figure). As scanning continues however, we get voltammogram with current same as bare Au electrode (Figure 5 b). In order to check whether there is any desorption of hydroxythiol monolayer that might have occurred during potential cycling in acetonitrile, we have carried out cyclic voltammetry with the same electrode which was already scanned in acetonitrile, in another redox system viz., 10 mM ferrocyanide in water containing 1 M KCl. Figure 6 (a) shows the cyclic voltammogram of bare gold electrode for ferrocyanide redox reaction in water with usual characteristics of a reversible redox process, while 6 (b) shows the CV of the same system which was subjected to potential scanning in acetonitrile. It can be seen that this electrode shows very good blocking to ferrocyanide redox reaction which is a clear indication that 11-mercapto 1-undecanol molecules are still existing on the gold surface. Next, we scanned the potential to a very negative value (below –1 V vs SCE) in acetonitrile, as it is known that the thiol monolayer desorbs at this potential. This electrode, after washing in millipore water, is cycled again in ferrocyanide containing

electrolyte and the CV (Figure 6 c) obtained clearly resembles that of bare gold electrode. The above series of experiments proves that neat 11-mercapto 1-undecanol monolayer was stable in acetonitrile medium within the potential range of scanning but undergoes some kind of disorganization which results in significant faradaic current during ferrocene redox reaction. These results are very much in agreement with our previous studies on the barrier properties of alkanethiol SAMs in different non-aqueous solvents [19]. Similar results were observed for neat 11-mercapto 1-undecanol coated gold electrode for the ferrocene redox reaction in propylene carbonate. Here, propylene carbonate can also disorganize the monolayer just like acetonitrile as both of these solvents lack solvent order through hydrogen bonding or dipole-dipole interaction. Since the solvent molecules are not bound to each other they are free to interact with the hydroxy group and methylene chain of the hydroxythiol monolayer and disorganize it.

Formamide

Figure 7 shows the cyclic voltammograms of hydroxythiol coated electrode with 1 mM ferrocene in formamide containing 0.1 M $LiClO_4$. The gold electrode was dipped in 1 mM 11-mercapto 1-undecanol in ethanol for 24 hours and the CV was carried out in 1 mM ferrocene in formamide containing 0.1 M $LiClO_4$. Figure 7a shows the CV with 1 mM 11-mercapto 1-undecanol coated electrode after a few cycles (around 20) and it is evident that the monolayer is fully disorganised even in a solvent like formamide, which has two-dimensional hydrogen bonded structure. This can be attributed to the strong interaction between the hydroxy group and formamide molecules through hydrogen bonding, which can weaken the lateral hydrogen bonding interactions between the terminal hydroxyl groups of neighbouring hydroxythiol molecules. This will disorganize the

monolayer adsorbed in ethanolic solution and allow the ferrocene redox reaction to take place through the disorganized monolayer, by the mechanism described earlier. However, the monolayer formed in neat thiol solution in absence of ethanol shows excellent blocking behaviour to ferrocene redox reaction in formamide (Figure 7b). This excellent blocking behaviour can be attributed to the strong lateral hydrogen bonding interactions between the terminal hydroxyl groups of neighbouring hydroxythiol molecules, so that the hydroxyl groups are not free to interact with the formamide molecules through hydrogen bonding.

Ethanol

Figure 8 shows the cyclic voltammograms of hydroxythiol coated electrode with 1 mM ferrocene in ethanol containing 0.1 M $LiClO_4$. It can be seen from the voltammogram that neat 11-mercapto 1-undecanol coated au electrode shows excellent blocking behaviour towards ferrocene redox reaction in ethanol (Figure 8b) compared to dilute ethanolic SAM of hydroxythiol (Figure 8a). The results in ethanol as electrolytic medium are similar to those observed in case of formamide. Both formamide and ethanol have some solvent order through hydrogen bonding. But it shows poor blocking behaviour in disorganizing solvents like acetonitrile and propylene carbonate.

11-mercapto undecanoic acid

Figures 9 and 10 illustrate the voltammograms of neat and 1 mM 11-mercapto undecanoic acid SAM coated gold electrode for ferrocene redox reaction in acetonitrile and formamide respectively. The blocking behaviour of 11-mercapto undecanoic acid SAM towards ferrocene redox reaction in acetonitrile and formamide is same as the hydroxythiol coated SAM. This is due to similar structure of hydroxythiol and carboxylic acid thiol SAMs, as

both are stabilized by lateral hydrogen bonding interactions between the terminal groups.

Hence, in terms of the ability to disorganise the hydroxy and carboxylic acid thiol monolayer, the solvents can be arranged in the order, propylene carbonate ≅ acetonitrile > ethanol ≅ formamide.

4.2.7 Effect of pH on the barrier properties of 11-Mercapto undecanoic acid and 4-amino thiophenol SAMs on gold

The main purpose of our studies on the barrier properties of ionic SAMs towards ionic electroactive species as a function of pH, is to understand the effect of surface charge on the terminal groups of the ionic SAMs on the electron transfer properties.

<u>11-mercapto undecanoic acid SAM</u>

Ruthenium (III) redox reaction

Figure 11 shows the reversible voltammogram of bare evaporated gold electrode for the ruthenium (III) redox reaction in 0.1 M $LiClO_4$.

In Figure 12, the cyclic voltammograms show the blocking behaviour of the 11-mercapto undecanoic acid SAM ($HSC_{10}COOH$) to $Ru(NH_3)_6^{3+}$ as a function of electrolyte pH (adjusted by adding H_2SO_4 or NaOH solution to an unbuffered electrolyte). The carboxylic acid SAM at a pH of 4.5 shows cathodic peak, but the anodic peak is absent (Figure 12 A). As the pH of the electrolyte solution containing ruthenium (III) is increased to 6 the cathodic and anodic peaks due to pinholes become visible and we observed quasi-reversible voltammogram with very large peak separation, but current almost same as bare gold electrode (Figure 12 B). Peaks due to cathodic and anodic current are visible in the pH range 6-8 (Figure 12 B-D). The current due to cathodic reaction is greater than the anodic current in all these cases.

To check whether the SAM is desorbed or damaged during the increase of pH of the electrolyte solution, we have reduced the pH of the electrolyte solution. Figure 12 F shows the voltammogram at a pH of 4.0. At this pH, the voltammogram shows very good blocking behaviour. Our results suggest that the SAM has not desorbed or damaged during the increase of pH. Our results can be explained as follows: The charge of the ionic monolayer terminal group will affect the distribution of the redox species near the electrode surface. The positively charged surface will attract the anionic species, whereas it repels the cationic species. Opposite effect is observed in case of negatively charged surface. The surface concentration of the electroactive species (C_s) is related to the bulk concentration (C_b) by the expression $C_s = C_b \exp(-zF\phi_{DL}/RT)$, where ϕ_{DL} is the electrical potential drop across the diffuse layer and z is the charge of the electroactive species. The poor blocking behaviour of 11-mercapto undecanoic acid SAM to ruthenium (III) redox reaction in pH range 6-8 can be attributed to electrostatic attraction of positively charged ruthenium redox species towards negatively charged carboxylic acid SAM (the carboxylic acid SAM starts to ionize at pH 5). At pH 4.5, a few –COOH groups start to ionize, but most of the –COOH groups remain unionized. At this pH, application of positive potential (for anodic reaction) will try to neutralize the slight negative charge attained by the ionization of a few –COOH groups. On the other hand, application of negative potential (cathodic reaction), the carboxylic acid SAM has slight negative charge. So at this pH, the carboxylic acid SAM exhibits better blocking behaviour towards anodic reaction compared to cathodic reaction of ruthenium (III) redox molecules. The applied potential (positive or negative potential) affects the charge on the terminal groups of the ionic carboxylic acid SAM. Between pH values 6

to 8, the complete ionization of the –COOH groups of the carboxylic acid SAM can take place. Hence, due to the effect of applied potential on the surface charge of ionic SAM, the cathodic current will be always greater than the anodic current.

Ferrocyanide redox reaction

Figure 13 shows the voltammograms corresponding to the blocking behaviour of 11-mercapto undecanoic acid SAM towards ferrocyanide redox reaction as a function of electrolyte pH (4-10). It can be seen at all pH values (4-10), the carboxylic acid SAM exhibits good blocking behaviour to ferrocyanide redox reaction (Figure 13 A-C). However, the faradaic current due to ferrocyanide redox reaction is lower in basic pH (Figure 13 A; pH=10) than in neutral (Figure 13 B; pH =7) or acidic pH (Figure 13 C; pH =4). At basic pH, the negatively charged carboxylic acid SAM repels negatively charged $[Fe(CN)_6]^{4-}$, which can be attributed to its excellent blocking behaviour. Similarly, neutral carboxylic SAM at acidic pH also shows good blocking behaviour to ferrocyanide redox reaction just like other uncharged SAMs.

<u>4-amino thiophenol (ATP) SAM</u>

Ferrocyanide redox reaction

Figure 14 shows the cyclic voltammograms of 4-amino thiophenol (ATP) SAM on gold for 10 mM ferrocyanide redox reaction in 1 M NaF as a function of electrolyte pH. At low pH, the SAM exhibits poor blocking behaviour to ferrocyanide redox reaction (Figure 14 A). The voltammogram shows cathodic and anodic peaks due to ferrocyanide redox reaction. However, as the pH of the electrolyte solution is enhanced, the ATP SAM shows very good blocking behaviour to ferrocyanide redox reaction with no peak current. The blocking behaviour of the ATP SAM changes reversibly

with electrolyte pH, as can be seen from the voltammograms. At a pH of 7, the amino group of ATP SAM starts to be protonated and become positively charged. However, at basic pH, when the ATP SAM becomes uncharged, it can block the ferrocyanide redox reaction like other uncharged SAMs.

Ruthenium (III) redox reaction

Figure 15 shows the voltammograms of ATP SAM for the ruthenium (III) redox reaction in 0.1 M $LiClO_4$ as a function of pH. At low pH, the ATP SAM exhibits poor blocking behaviour to ruthenium (III) redox reaction (Figure 15 A). This is rather surprising, as we expect the positively charged ATP SAM to impede the ruthenium (III) redox reaction due to electrostatic repulsion. However, on increasing the pH of the solution, the redox reaction is gradually impeded as can be observed from the decrease in current in the voltammogram (Figure 15 C-D). Probably, the effect of charge of the monolayer on the faradaic reaction of electroactive species become unimportant for shorter chain thiol monolayer like 4-amino thiophenol. At basic pH, there is strong lateral hydrogen bonding interactions between the terminal uncharged NH_2 groups of the neutral ATP SAM, which is responsible for the excellent blocking behaviour of ATP SAM towards both ferrocyanide and ruthenium (III) redox reactions. At low pH, the NH_2 terminal group is protonated and probably there is strong ionic repulsion between the terminal NH_3^+ groups of the ATP SAM. This effect can weaken the lateral hydrogen bonding interaction and thus disorganize the SAM. This disorganization makes the blocking behaviour of ATP SAM poor towards the ruthenium (III) and ferrocyanide redox reactions.

4.3 Conclusions :

<u>The following conclusions can be inferred from our work :</u>

1. From the measurements of interfacial capacitance values for dithiol coated gold surface, it can be inferred that the dithiol molecules are most likely to be adsorbed with only one sulphur atom bonded to gold resulting in a vertical orientation.
2. From our cyclic voltammetry and impedance studies with ferrocene redox probe in acetonitrile, we conclude that BDMT molecules can form more organized monolayers on gold than aliphatic octanedithiol SAMs due to extremely strong lateral van der Waals interaction among the phenyl rings.
3. The barrier properties of the hydroxy and carboxylic acid thiol SAMs in different electrolytic non-aqueous solvents are related to both the structure of the thiol monolayers and solvents. Hence, in terms of the blocking behaviour of the hydroxy and carboxylic acid thiol monolayers to ferrocene redox reaction, the solvents can be arranged in the order, formamide ≅ ethanol > propylene carbonate ≅ acetonitrile.
4. Blocking behaviour of ionic SAMs towards ionic electroactive species depends on the pH of the electrolytic solution and applied potential.

a) We find that 11-mercapto undecanoic acid SAM exhibits poor blocking behaviour towards ruthenium (III) redox reaction at low pH, but shows excellent blocking behaviour at high pH. On the other hand, the same monolayer shows excellent blocking behaviour to ferrocyanide redox reaction even at low pH. The effect of charge of the ionic carboxylic acid thiol plays important role in the blocking behaviour towards redox reactions involving ionic electroactive species.

b) The ATP SAM shows poor blocking behaviour towards ferrocyanide and ruthenium (III) redox reaction at low pH, but shows good blocking behaviour at high pH. In this case, the effect of charge of the ionic SAM becomes unimportant for short chain length thiol SAM like ATP. In this case, the structure of ATP SAM will determine the barrier property, which will change with the pH of the electrolytic solution. The lateral hydrogen bonding interaction between the terminal NH_2 groups of the ATP SAM will determine the structural integrity and hence the blocking behaviour towards ionic electroactive species.

REFERENCES

1. R.G.Nuzzo, D.L.Allara, *J.Am.Chem.Soc.*, 105 (1983) 4481
2. R.G.Nuzzo, B.R.Zegarski, L.H.Dubois, *J.Am.Chem.Soc.*, 109 (1987) 733
3. M.D.Porter, T.B.Bright, D.L.Allara, C.E.D.Chidsey, *J.Am.Chem.Soc.*, 109 (1987) 3559
4. H.O.Finklea, S.Avery, M.Lynch, R.Furtsch, *Langmuir*, 3 (1987) 409
5. E.B.Troughton, C.D.Bain, G.M.Whitesides, R.G.Nuzzo, D.L.Allara, M.D.Porter, *Langmuir*, 4 (1988) 365
6. D.L.Allara, R.G.Nuzzo, *Langmuir*, 1 (1985) 45
7. R. Moaz, J.Sagiv, *Langmuir*, 3 (1987) 1034
8. E.Sabatini, I.Rubinstein, R. Moaz, J.Sagiv, *J.Electroanal.Chem.*, 219 (1987) 365
9. E.Sabatini, I.Rubinstein, *J.Phys.Chem.*, 91 (1987) 6663
10. H.O.Finklea, D.G.Hanshew, *J.Am.Chem.Soc.*, 114 (1992) 3173
11. C.E.D.Chidsey, *Science*, 251 (1991) 919
12. C.E.D.Chidsey, C.R.Bertozzi, T.M.Putvinski, A.M.Mujsee, *J.Am.Chem.Soc.*, 112 (1990) 4301
13. C.Miller, P.Cuendet, M. Gratzel, *J.Phys.Chem.*, 95 (1991) 877
14. C.Miller, M. Gratzel, *J.Phys.Chem.*, 95 (1991) 5225
15. A.M.Becka, C.J.Miller, J.Phys.Chem., 96 (1992) 2657
16. C.D.Bain, E.B.Troughton, Y.T.Tao, J,Evall, G.M.Whitesides, R.G.Nuzzo, *J.Am.Chem.Soc.*, 111 (1989) 321
17. R.G.Nuzzo, L.H.Dubois, D.L.Allara, *J.Am.Chem.Soc.*, 112 (1990) 558
18. C.E.D.Chidsey, D.N.Loiacono, *Langmuir*, 6 (1990) 682
19. U.K.Sur, V.Lakshminarayanan, *J. Electroanal. Chem.*, 516 (2001) 31

20. U.K.Sur, V.Lakshminarayanan, *Proc.of seventh International Symposium on Advances in Electrochemical Science and Technology*, SAEST, CECRI, INDIA, 27-29 November, Chennai, 2002, p B1-B4
21. *Molecular Electronics: Science and Technology*, A.Aviram, (Ed.), Confer. Proc. No. 262, American Institute of Physics, New York, 1992
22. J.M. Tour, R. Wu, J.S. Schumm, *J.Am.Chem.Soc*., 113 (1991) 7064
23. *Nanostructure Physics and Fabrication*, M.A.Reed, W.P. Kirk, (Eds.), Academic Press, New York, 1989
24. *Nanostructures and Mesoscopic Systems*, M.A.Reed, W.P. Kirk, (Eds.), Academic Press, New York, 1992
25. M. Brust, P.M. Blass, A.J. Bard, *Langmuir*, 13 (1997) 5602
26. H.Riley, G.K. Kendall, F.W. Zemicael, T.L.Smith, S.Yang, *Langmuir* 14 (1998) 5147
27. T.Nakamura, H. Kondoh, M.Matsumoto, H. Nozoye, *Langmuir*, 12 (1996) 5977
28. K. Kobayashi, T. Horiuchi, H.Yamada, K. Matsushige, *Thin Solid Films*, 331 (1998) 210
29. U.K.Sur, R.Subramanian, V.Lakshminarayanan, *J.Colloid Interface Sci.*, (Submitted)
30. K.Doblhofer, J.Figura, J.H.Fuhrhop, *Langmuir*, 8 (1992) 1811
31. K.Takehara, H.Takemura, Y.Ide, *Electrochim Acta*, 39 (1994) 817
32. C.P.Smith, H.S.White, Langmuir, 9 (1993) 1
33. H.O. Finklea, *Electrochemistry of Organized Monolayers of Thiols and Related Molecules on Electrodes*, A.J.Bard and I.Rubinstein (Eds.), Marcel Dekker, New York, 1996, p 208
34. A.Fitch, D.H.Evans, *J.Electroanal.Chem.*, 202 (1986) 83
35. D.O.Wipf, R.M.Wightman, *Anal.Chem.*, 60 (1988) 2460

36.R.A.Malsmsten , C.P.Smith, H.S.White , *J.Electroanal.Chem.*,215 (1986) 223

37.Proceedings of the symposium on Electrochemical Capacitors II , F.M. Delnick, D. Ingersoll, X.Andrieu, and K. Naoi, (Eds.), Volume 96-25, The Electrochemical Society, New Jersey, 1997, p 222

38.P. Zoltowski, *J. Electroanal.Chem.*, 443 (1998) 149